Equivalent Circuit Models for Propagation Analysis of In-Building Power line Communications Systems

Azlan Hakimi and Grant A. Ellis

Department of Electrical and Electronics Engineering
Universiti Teknologi Petronas, Tronoh, Perak 31750, Malaysia
azlan.hakimi@yahoo.com and grant.ellis@gmail.com

Abstract ─ In-building power line transmission measurements show potential for low attenuation propagation above 30 MHz. These measurements show that frequency bands can exist having low or minimum attenuation above 100 MHz. A simple high-frequency propagation model for analysis of in-building communications up to 900 MHz, which can be implemented using a commercial circuit simulator, is described. This physics-based model is extracted using broadband data from both time- and frequency-domain network transmission (S_{21}) measurements. The novelty of this modeling approach is that different propagation modes such as electromagnetic coupling, waveguide propagation through the wiring conduit, and fading are included. An RF circuit model in a simulator environment is useful for analyzing a wide range of communication problems at the circuit, subsystem, and system levels.

Index Terms - Frequency response, modeling, power line communications, propagation, transmission line, and waveguide.

I. INTRODUCTION

The power line network is a low-cost alternative to existing wired and wireless systems for wideband or broadband data communications. Broadband power line communications (PLC) is a system that uses existing power distribution lines and is characterized by a carrier system connected to power lines to transmit radio frequency signals for broadband communications. PLC is an alternative mode of communication and differs from other wired and wireless systems and is preferred due to the wide availability and easy implementation using the existing power line networks in a designated area [1, 2]. PLC was initially used as a remote monitoring system in the high voltage portion of the power line system for unmanned sites for the purpose of controlling and monitoring the power network [3]. One of the main uses of PLC is carrier transmissions over power line (CTP), which covers three basic functions including operations management, electric line monitoring and limitation, and removal of failures [4]. It is gradually being applied to the medium and low voltage lines especially in home networks due to the wide availability of power lines [5, 6]. This is due to the existing power line system, which can greatly reduce the cost of deploying a new communication system since it does not require additional infrastructure. Another advantage is that it can penetrate areas that are remote or rural and do not have a readily available connection [4, 7]. A number of research trials have been carried out at different locations and show that broadband power line is a possible technique for data communications [8–11].

Most of the PLC research to date only covers the frequency band up to 30 MHz [12]. Although this is sufficient at present, it is necessary to increase the transmission rates due to the requirements for higher data rates and higher speed. Since the introduction of PLC there has been promising research for evaluation at frequencies above 30 MHz [5]. Commissions and regulatory bodies around the world such as the federal communications commission (FCC) have set up guidelines and regulations for operators regarding broadband PLC [12]. It is stated in the FCC guidelines that frequencies above 40 MHz

Submitted On: Aug. 11, 2012
Accepted On: Mar. 28, 2013

requires further research and development. In [13], a technique to provide Wi-Fi coverage to users within a physical or "fenced" boundary is proposed. Power line communications can be utilized to perform the same purpose since it supports relatively short distances such as in a room or on an office floor. A model of the PLC channel transfer function is derived for the frequency range of 1 MHz to 30 MHz by using a two-wire transmission approximation and derivation of characteristic impedance and propagation constant are done analytically [14, 15]. A broadband power line model based on transmission line theory is validated by comparing transfer function response with actual measurements for frequencies up to 100 MHz. Above 30 MHz, the experimental and modeled results begin to deviate [16]. The power line network is modeled using a multiconductor transmission line and the network is simulated with ABCD matrices. The results are however, validated using a laboratory setup and do not use an actual power line system [17, 18].

The focus of this paper is to develop a model, which can be used to evaluate the feasibility of higher frequency broadband PLC circuits and systems. This model is useful for simulating circuit configurations in a PLC environment. Since the model is physics-based, effects such as time delay, multipath, and dispersion are included. This model is broadband so that effects at harmonic frequencies can also be simulated. Time-varying effects such as fading can also be included using random simulation of varying attenuation in the model.

To develop a model for PLC for use above 30 MHz, in-building measurements were taken to determine the transmission parameters (S_{21}) of the network. The neutral line was chosen instead of the phase line for transmission because it is believed to have less loading and to minimize the presence of high voltage on the measurement equipment [19]. Different locations and times of the day were chosen for measurements. From the measured data, it is shown that potential PLC systems have significant attenuation and that the transmission characteristics can vary significantly during the day. Electric field emission measurements were also taken and to comply with FCC specifications, the input power to the PLC must be limited to keep the emissions to acceptable levels [20]. The broadband propagation model is fitted to measured data, which can be implemented using Agilent ADS [21]. The availability of an RF model in a circuit simulator environment is especially useful for analyzing a wide range of communications problems at the circuit, subsystem, and system levels.

This paper is organized as follows: section II describes the methodology used for measurements, section III describes the measurement results, section IV describes the methodology for extraction of an equivalent RF circuit model for the PLC, and finally the paper is concluded.

II. MEASUREMENT METHODOLOGY AND CONFIGURATION

The in-building power line system is utilized by exciting the neutral and ground lines in a transmission line mode where the signal is fed into the neutral line and the ground is used as the signal return. The neutral and ground run separately as parallel wires and are connected only at the incoming service main circuit breaker or transformer. In order to develop the broadband models for in-building power line system, S_{21} (transmission) parameter measurements were carried out to determine the attenuation and return loss. These measurements were taken using a network analyzer and include high pass filters connected to the neutral and ground using shielded cables at the power sockets in the measurement setup shown in Fig. 1.

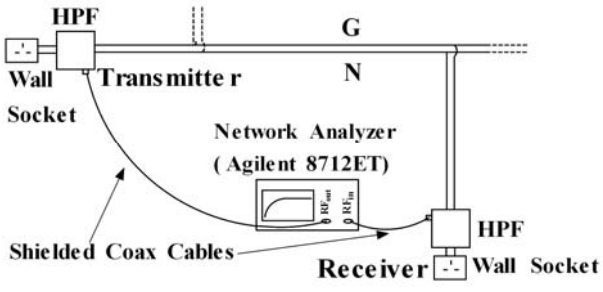

Fig. 1. S_{21} transmission measurement setup.

The high pass filters have a cutoff frequency of 5 MHz and are located at each end of the path. The filters are necessary to protect the measurement equipment since the power line network is constantly active and supports many loads including lighting, air conditioning, computers, printers, and elevators all of which can

contribute noise, transients, and even faults in the power system. The high-pass filter schematic diagram is shown in Fig. 2. The high pass filter circuit with the power socket is shown in Fig. 3.

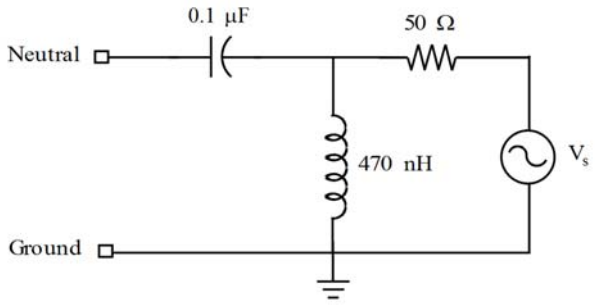

Fig. 2. High-pass filter used for isolating measurement equipment.

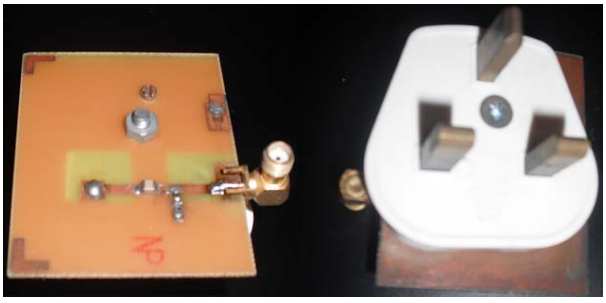

Fig. 3. High pass filter circuit (top and bottom socket).

Several locations in building Block 22 at Universiti Teknologi Petronas located in Tronoh Malaysia were chosen for these measurements. Block 22 has four floors including the ground and was constructed in 2003. Path A in room 22-02-02 has a length of 11 m (in the same room), path B is in room 22-02-02 with approximate length of 9 m (from inside to outside of the room), path C is in room 22-02-05 with approximate length of 6 m (from inside to outside of the room), path D is in room 22-02-02 with approximate length of 3 m (in the same room), and path E is from Wing 1 to Wing 2 with approximate length of 45 m. There are several panels distributed nearly evenly throughout each wing. All of the ground, neutral, and phase lines in each room pass through a PVC duct and are collected at the panel located adjacent to that room. These panel locations are shown in the diagram in Fig. 4. All of the ground, neutral, and phase lines from the panels then pass through an overhead metallic conduit to the end of each wing to the riser.

The simulated and measured transmission (S_{21}) and reflection (S_{11}) coefficients for the high pass filter for Z_0 = 50 Ω are shown in Fig. 5. The measured insertion loss for the filter is less than 4 dB below 0.8 GHz. Also shown in the figure is the return loss (Γ) of the high pass filter connected to the power line network. The measured return loss is better than 10 dB for several frequencies below 500 MHz.

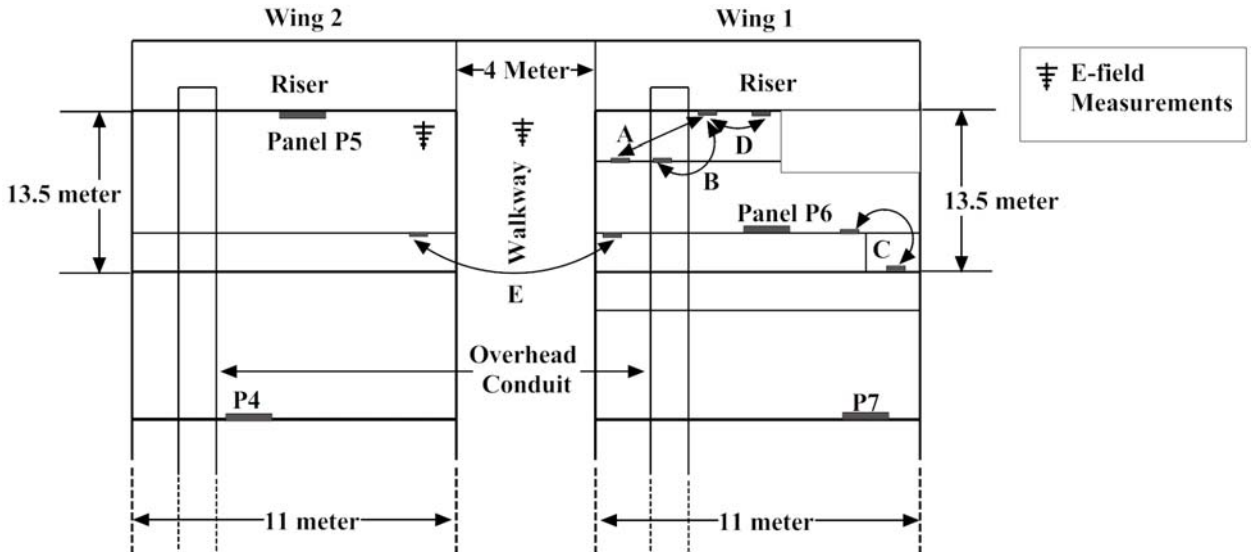

Fig. 4. Building diagram for paths A, B, C, D, and E.

The neutral-ground transmission line configuration has an average input impedance of about 70 Ω. The filters were connected to the wall socket and the transmission parameters (S_{21}) were measured using a calibrated Agilent 8712ET network analyzer. As will be evident in the S_{21} measurements, as the path length increases, the received signal attenuates and a power amplifier is required to increase the transmission of the system. The field measurements were carried out by injecting RF signals into the power line through a power amplifier and high pass filter and the field emissions were measured using an AFJ EBA-01 log periodic dipole and an Advantest R3132 spectrum analyzer located a distance of 3 meters from the power line feed points (Fig. 6).

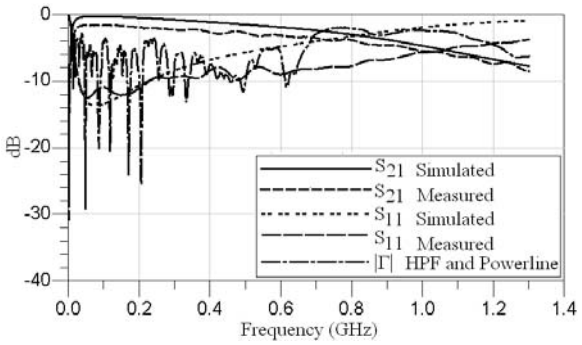

Fig. 5. S_{21} and S_{11} for the high pass filter (Z_0 = 50 Ω).

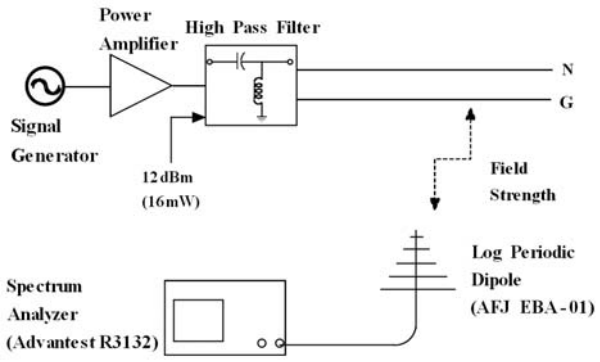

Fig. 6. Electric field measurement setup.

III. MEASUREMENT RESULTS

In this section, the measurement setup described in the previous section is used to measure the transmission coefficient S_{21} for the paths shown in Fig. 4. The measurements were taken at 10 am, 12 pm, 3 pm, 5 pm, and 8 pm over a span of nearly one month to determine the attenuation and amount of fading in the PLC. Broadband measurements were taken to estimate the impulse response of the power line system. Field probe measurements were taken and the results are compared with the transmission data to identify any possible coupling. In the next section, this measurement data is used to extract an equivalent RF circuit model of the power line system.

A. Different times of day

The measured S_{21} for paths A, B, and E are shown in Figs. 7 - 9. The response for each path shows that the transmission can vary with the time of the day and that a frequency band having minimum attenuation or resonance exists between 400 MHz and 700 MHz. This is strongly evident in path A and path E at different times of the day while for path B the location of the resonance is nearly constant. The measurement data shown in Figs. 7 and 8 were measured at 5 pm on separate days for both paths and show almost no difference in resonance frequency. The electrical line loads vary at different times, which also affect the RF S_{21} transmission.

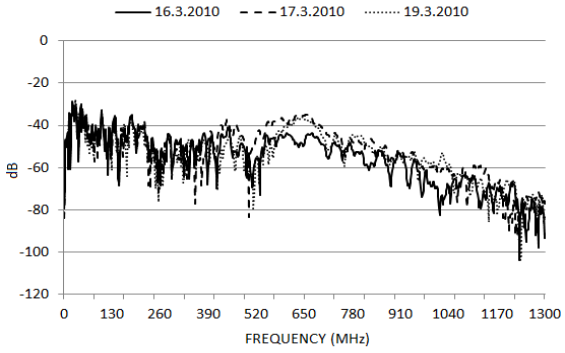

Fig. 7. S_{21} measured at 5pm on separate days for path A.

At 5 pm, the S_{21} measured for path A shows resonance between 400 MHz and 500 MHz and between 500 MHz and 715 MHz. The measurement for path B shows nearly constant S_{21} from 400 MHz to 715 MHz with the exception of a slight variation in the peak in the range of 600 MHz to 715 MHz. The wing-to-wing (path E) measurements in Fig. 9 show a peak in S_{21} between 244 MHz and 650 MHz. The maximum variation in the measured S_{21} or fading is about 20 dB. In each case the resonant frequency range is nearly constant.

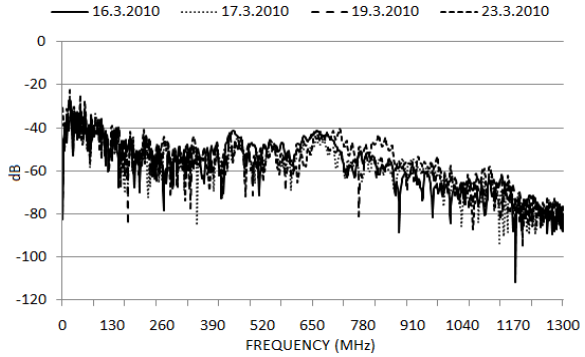

Fig. 8. S_{21} measured at 5pm on separate days for path B.

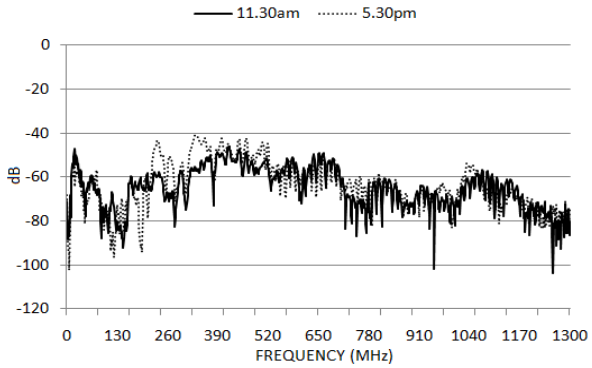

Fig. 9. S_{21} measured at different times for path E.

B. Field emission measurements

The average measured transmission, S_{21} for path E (wing to wing) and electric field intensity near the center of the walkway are shown in Fig. 10. The field probe is located at a distance of 3 meters from the input to the power line (see Fig. 4). The input power to the high pass filter is 16 mW. These measurements reveal that there is a correlation between peaks in both S_{21} and the resulting electric field intensity. For some frequencies e.g. 450 MHz there is both low attenuation in S_{21} and a minimum field emission level.

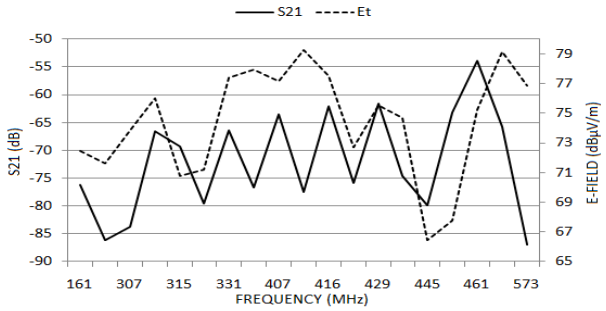

Fig. 10. S_{21} and electric field measurements (161 MHz to 572.5 MHz).

The measured total electric field levels are higher than permitted by FCC (40 dBµV/m for frequencies above 40 MHz) and are due to the configuration of the power line network in the building. Here, asymmetries in distribution of the neutral and ground lines generate common mode currents resulting in radiation [20]. Simply lowering the input power to the PLC however, can lower these emission levels. The measured input power to the high pass filter required to maintain a field emission of 40 dBµV/m is only -15 dBm at 700 MHz. From the FCC and other commission guidelines, frequencies above 40 MHz are subjected to further development and deployment scenarios.

C. Frequency response and estimation of impulse response of power line system

The measurement setup described in the previous section and shown in Fig. 1 was also used to estimate the impulse response of the PLC. The data was obtained for the transmission paths in Block 22 (Fig. 4). The S_{21} was first measured for each path and then converted into real and imaginary parts. The frequency range used was 0.3 MHz to 1.3 GHz. Next, the data was loaded into MATLAB^{TM} [22] and expanded by using complex conjugation into a set of positive and negative frequencies. Finally, the data was inverse fast Fourier transformed using the IFFT command to estimate the (real) impulse response.

Figure 11 is the original transmission (S_{21}) magnitude data in frequency domain and Fig. 12 is the estimated impulse response for path A. A number of reflections are present on the line and from 400 MHz – 600 MHz there is a small increase in S_{21}. This is believed to be primarily due to the conduit. Figure 13 is the original transmission (S_{21}) magnitude data in frequency and Fig. 14 is the impulse response for path B. For this path, there are also several reflections present and another small peak in S_{21} occurs near 600 MHz. Figure 15 – 18 are the original transmission (S_{21}) magnitude data in frequency and impulse response for paths C and D.

Transmission paths C and D have the shortest path lengths or propagation distances and have the fewest reflections. Figure 16 (path C) response shows that the signal is damped for $t > 200$ nsec. Figure 18 (path D) response shows that the signal is damped for $t > 75$ nsec. The time required for

the reflections to decay is inversely proportional to the path length. Path C and path D have a shorter distance compared to path A, B, and E, which show the least damping.

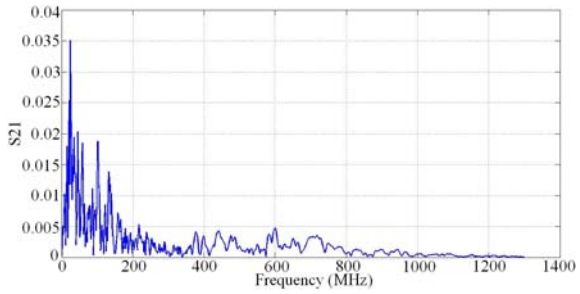

Fig. 11. Frequency magnitude response for transmission path A.

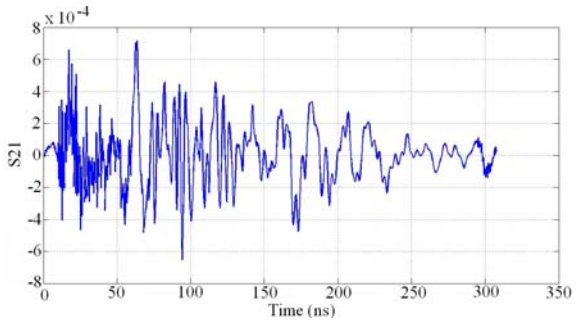

Fig. 12. Impulse response for transmission path A.

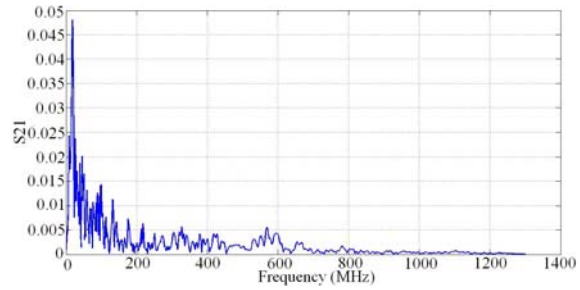

Fig. 13. Frequency magnitude response for transmission path B.

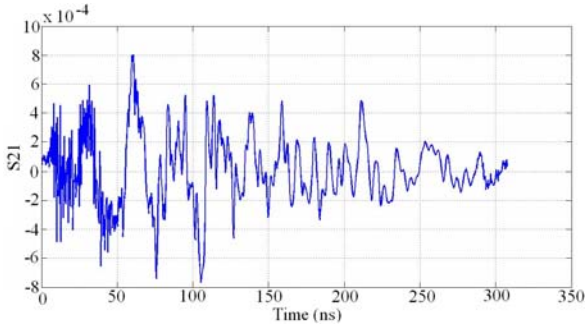

Fig. 14. Impulse response for transmission path B.

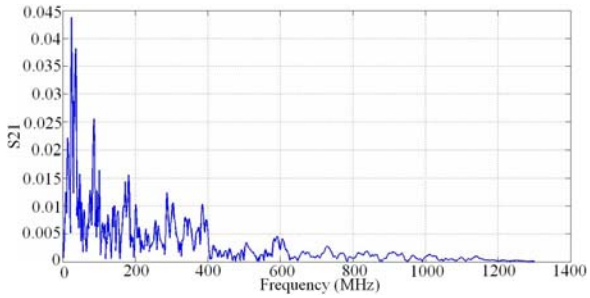

Fig. 15. Frequency magnitude response for transmission path C.

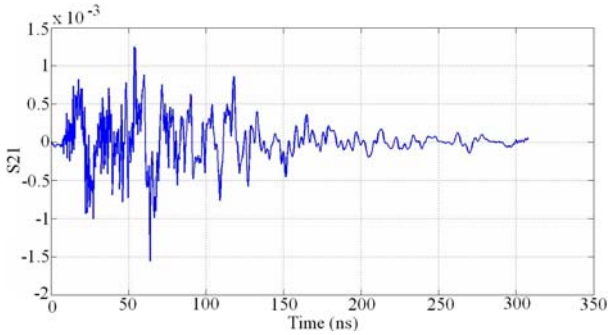

Fig. 16. Impulse response for transmission path C.

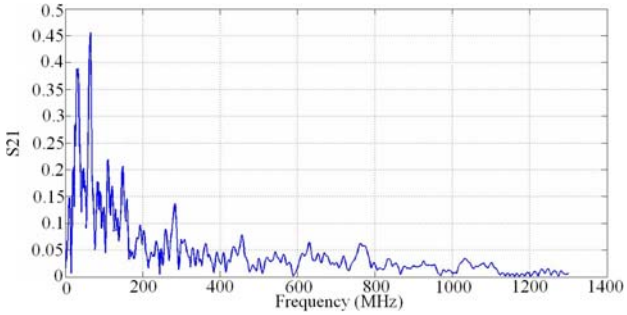

Fig. 17. Frequency magnitude response for transmission path D.

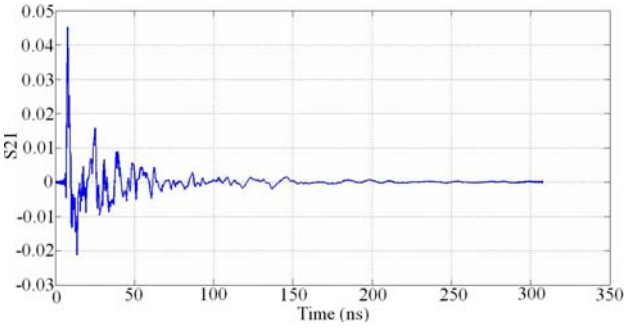

Fig. 18. Impulse response for transmission path D.

Figures 19 and 20 show the S_{21} responses for path E (wing to wing). Figure 19 is the measured transmission (S_{21}) magnitude data in frequency domain and Fig. 20 is the estimated impulse response. Figure 20 shows damping in the signal and some reflections and a peak at t = 280 nsec. In the frequency response, above 400 MHz there are several peaks. The corresponding impulse response shows peaks at 30 and 280 nsec. These peaks can be identified as direct electromagnetic coupling between the two wings and a high frequency waveguide mode due to propagation through the conduit.

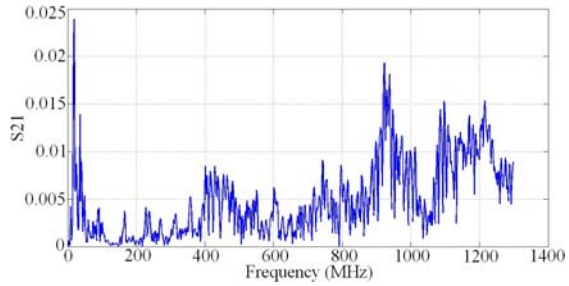

Fig. 19. Frequency response for transmission path E (wing to wing).

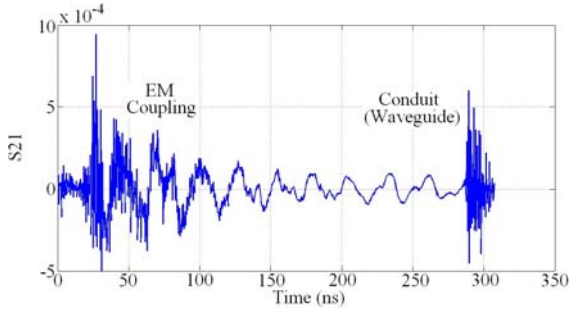

Fig. 20. Impulse response for path E (wing to wing).

Field probe measurements were taken to provide further insight into electromagnetic coupling into the power line. Figure 21 shows the measured S_{21} for the wing-to-wing (path E) wall socket to wall socket (N-G to N-G) and wing-to-wing wall socket (N-G) to a field probe located adjacent to the second wall socket. The distance between the field probe and first wall socket is 9 m. The wall socket to wall socket transmission data (N-G to N-G) shows both low and high frequencies present (> 400 MHz). From the field probe measurement data, low frequencies couple the most and the high frequency data is not present. Figure 22 shows the corresponding time domain wing-to-wing measurements. Comparison of the impulse response for wall socket to wall socket and wall socket to field probe show that propagation through the ground-neutral lines for t > 250 nsec is due to the waveguide mode in the conduit only. Also, the field probe measurements show a response for t > 28 nsec, which suggests coupling from the wall socket. From the foregoing analysis of the frequency- and time-domain responses, the primary propagation components through the power lines are direct electromagnetic coupling and a waveguide mode through the conduit.

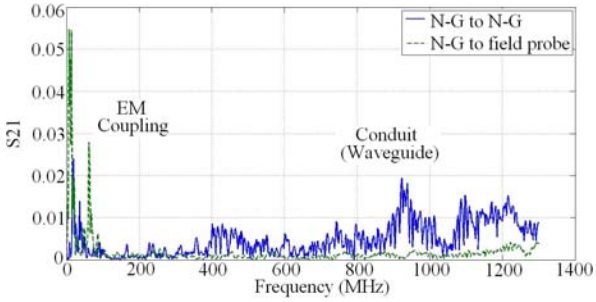

Fig. 21. Frequency response for transmission path E (wing to wing): direct and field probe.

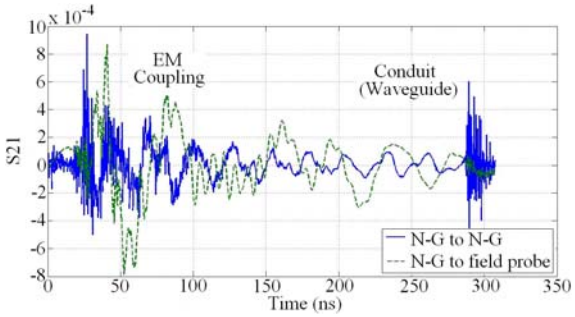

Fig. 22. Impulse response for transmission path E (wing to wing): direct and field probe.

IV. EQUIVALENT RF CIRCUIT MODEL FOR POWER LINES

During measurement of the power line network in the previous section, it was observed that there could be several transmission paths. There is a direct path and additional paths that result in reflections. When the source and receiver are located in different wings, electromagnetic (EM) coupling can also occur. Also, the signal can propagate in modes other than the neutral-ground

(TEM) type mode. In Block 22 for distances greater than 5 meters, the wires must travel through an overhead conduit where the transmission coefficient (S_{21}) can increase instead of decrease with frequency. At certain frequencies, this increase in S_{21} was found to be caused by exciting a waveguide mode inside the conduit. From the dimensions of the conduit, it was calculated that the waveguide cutoff frequency for the lowest order TE_{10} mode is about 750 MHz. For other locations where the path length is less than 5 meters and the wires do not pass through a conduit (waveguide) the S_{21} shows a response that decreases monotonically with frequency.

For power line connections with path lengths greater than 5 meters and where the neutral and ground lines pass through a conduit, a simple model was developed using ADS™ and CST™ [23] to estimate the power distribution between the conduit represented by TE_{10} mode and the neutral-ground wires represented by the TEM mode. This model decomposes the propagation into TEM and TE_{10} propagating modes and is shown in Fig. 23.

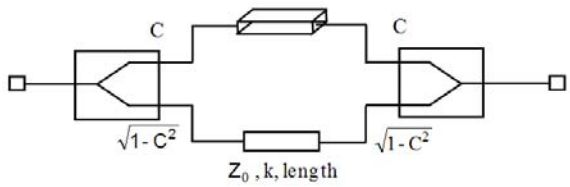

Fig. 23. Equivalent circuit model for propagation through conduit.

To create the conduit model for implementation in a circuit simulator such as ADS™, a numerical procedure was first used to estimate the coupling (C) for 2-wire transmission through a rectangular waveguide. The power coupled into each mode is conduit = C, and for the neutral-ground wires = $\sqrt{(1-C^2)}$. For the model, parameters varied are the spacing (d) between the 2 wires and the height (h) of the wires inside the waveguide as shown in Fig. 24. Simulations were carried out with varying parameters d and h using CST™ and the resulting coupling parameter value C was extracted. In the simulations, the conduit length is 5 meters and wire diameters are 1 mm. The values for Z_0 and k (relative dielectric constant) used in the transmission line model are assumed to be 200 Ω and 1.8. The spacing (d) and the height (h) are varied and simulated accordingly. The neutral and ground wires inside the conduit with spacing, d are varied between 1 and 5 cm. The estimated coupling, C is extracted using the following procedure:

1. Set the d and h values.
2. EM-simulate the structure shown in Fig. 24 from 0.3 MHz to 900 MHz using CST™.
3. Import the resulting S-parameters into the circuit simulator.
4. Fit the S-parameters to the circuit shown in Fig. 23 to extract C value.

For height (h) value of 0.1 mm, the value for C is lowest since the neutral and ground wires are placed near the bottom of the conduit and become nearly short-circuited. The coupling value C for this work occurs for the neutral and ground located at least 10 mm from the bottom of the conduit and the neutral and ground are spaced at least 20 mm apart. When the height (h) is 10 mm to 20 mm and spacing (d) is 20 mm to 50 mm, the range for the coupling, C is $0.18 < C < 0.23$.

A frequency dependent coupling can also be used. Here, the coupling increases with frequency and has the form $C = \alpha f$ where f is frequency. Using the procedure described above $\alpha = 0.6 - 0.8$ GHz^{-1} for the height (h) between 10 mm and 20 mm and spacing (d) between 20 mm and 50 mm.

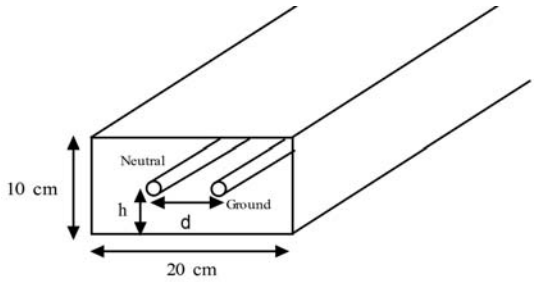

Fig. 24. Conduit cross-sectional view including neutral and ground.

From the layout given in Fig. 4, the equivalent RF circuit model for the wing-to-wing path consists of high pass filters at the transmitter and receiver, an equivalent circuit model for the conduit in each wing, a transmission line for the riser that connects both wings, and a short section of high attenuation transmission line used to model the coupling between the wings. Frequency dependant coupling between the TEM and TE_{10} modes in the conduit is included using $\alpha = 0.7$ GHz^{-1}. Figure 25 shows the equivalent circuit

propagation model for path E for implementation using ADS^{TM}. The final component values are determined by optimizing the model parameters with the frequency- and time-domain S_{21} data using ADS^{TM}. Time-varying attenuation or fading can be included in the model for random or Monte Carlo type analysis by varying the transmission line "*atw*" parameter. For 20 dB variation in attenuation, the range $0.4 < atw < 0.8$ is used.

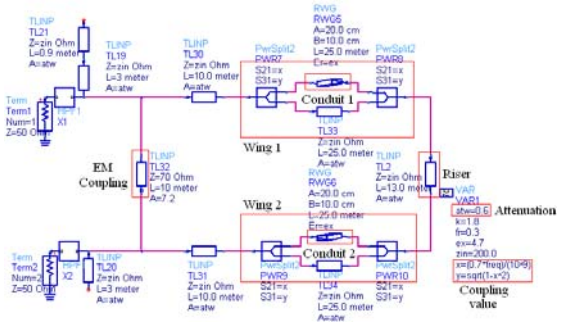

Fig. 25. ADS Schematic diagram for path E (wing to wing).

Figure 26 shows the measured and simulated S_{21} for the wing-to-wing transmission in the frequency- and time-domains. The measured data and simulated model compare well in both domains. For wing-to-wing transmission, the signal propagates through two conduits and the riser as well as direct coupling between the wings and is evident in the time domain response at 28 nsec and 290 nsec in Fig. 26 (b). Figure 26 (a) shows that the frequency response for measurement and simulation are similar up to 900 MHz. As mentioned earlier, the response for frequencies above 400 MHz is primarily due to the TE mode excited in the conduits.

V. CONCLUSION

The transmission measurements in an office building at different locations and times show that the power line system can have low attenuation for frequencies above 30 MHz. These measurements show that frequency bands exist that are nearly fixed with only 40 – 50 dB attenuation and maximum variation of 20 dB. Field strength measurements of the broadband power line were taken and demonstrate that in order to not exceed field levels required by FCC regulations, a low input power level must be used. A simple broadband propagation model for analysis of the PLC up to 900 MHz is extracted by using both frequency- and time-domain representations of the measured S_{21} parameters. Analysis of S_{21} in both domains is not only helpful in fitting the measured response to a useful model but is also helpful in identifying the various propagation modes. The RF propagation model can be implemented using a standard circuit simulator and provide a unified analysis capability for in-building PLC at the component, sub-system, and system levels. The model is easily modified to account for fading.

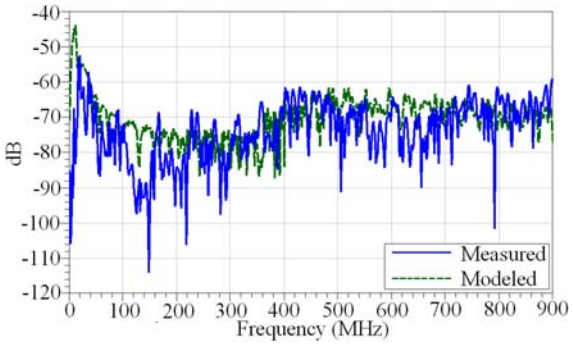

(a) Frequency response.

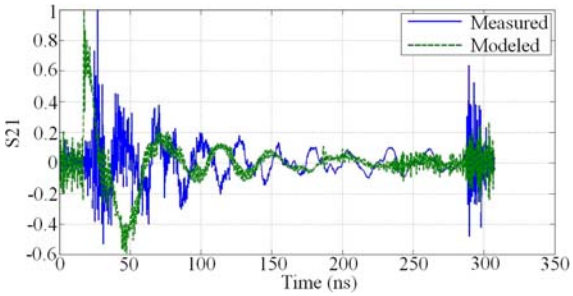

(b) Impulse response.

Fig. 26. Comparison of measured versus modeled S_{21} for path E (wing to wing).

REFERENCES

[1] A. Papaioannou and F. N. Pavlidou, "Evaluation of power line communication equipment in home networks," *IEEE Systems Journal*, vol. 3, no. 3, pp. 288-294, Sept. 2009.

[2] N. A. Pavlidou, H. Vinck, J, Yazdani, and B. Honary, "Power line communications: state of the art and future trends," *IEEE Commun. Mag.*, vol. 41, pp. 34-40, 2003.

[3] K. Dostert, *Power Line Communications*, Prentice Hall PTR, NJ, Upper Saddle River , pp. 1-2, 2000.

[4] S. Ntuli, H. N. Muyingi, A. Terzoli, and G. S. V. R. K. Rao, "Power line networking as an

alternative networking solution: A South African experience," *IEEE Power India Conference*, 2006.
[5] S. Chen, M. Setta, X. Chen, and C. G. Parini, "Ultra wideband power line communication (PLC) above 30 MHz," *IET Comm.*, vol. 3, no. 10, pp. 1587-1596, 2009.
[6] R. G. Olsen, "Technical considerations for wideband power line communication," *IEEE Power Engineering Society Summer Meeting*, vol. 3, pp. 1186-1191, Feb. 2002.
[7] D. Fink and R. J. Jaeung, "Feasible connectivity solutions of PLC for rural and remote areas," *IEEE Int. Sym. on Power Line Comm. and Its Appl.,* pp. 158-163, 2008.
[8] Y. J. Yang and C. M. Arteaga, "Broadband over power line field trial for commercial in-building application in a multi-dwelling-unit environment," *IEEE Int. Sym. on Power Line Comm. and Its Appl.*, pp. 342-346, 2009.
[9] C. M. Arteaga and Y. J. Yang, "Large scale broadband over power line field trial on medium voltage overheard circuits," *IEEE Int. Sym. on Power Line Comm. and Its Appl.*, pp. 289-292, 2008.
[10] T. Esmailian, F. R. Kschischang, and P. G. Gulak, "Characteristics of in-building power lines at high frequencies and their channel capacity," *IEEE Int. Sym. on Power Line Comm. and Its Appl.*, pp. 52-59, 2000.
[11] H. Philipps, "Performance measurements of power line channels at high frequencies," *IEEE Int. Sym. on Power Line Comm. and Its Appl.*, pp. 229-237, March 1998.
[12] A. Leimer and S. Martin, *Carrier Current Systems (CCS) and Broadband over Power Line (BPL)*, Office of Engineering and Technology, FCC Laboratory, May 2004.
[13] A. Sheth, S. Seshan, and D. Wetherall, "Geo-fencing: confining Wi-Fi coverage to physical boundaries," *Proc. Pervasive*, pp. 274-290, 2009.
[14] H. Meng, S. Chen, Y. L. Guan, C. L. Law, P. L. So, E. Gunawan, and T. T. Lie, "A transmission line model for high-frequency power line communication channel," *International Conference on Power System Technology*, vol. 2, pp. 1290-1295, 2002.
[15] H. Meng, S. Chen, Y. L. Guan, C. L. Law, P. L. So, E. Gunawan, and T. T. Lie, "Modeling of transfer characteristics for the broadband power line communication channel," *IEEE Trans. on Power Delivery*, vol. 19, no. 3, pp. 1057-1064, July 2004.
[16] J. Anatory, N. Theethayi, R. Thottappillil, M. M. Kissaka, and N. H. Mvungi, "An experimental validation for broadband powerline communication (BPLC) model," *IEEE Trans. on Power Delivery,* vol. 23, no. 3, pp. 1380-1383, July 2008.
[17] T. Banwell and S. Galli, "A novel approach to the modeling of the indoor power line channel-Part I: circuit analysis and companion model," *IEEE Trans. on Power Delivery*, vol. 20, no. 2, pp. 655-663, 2005.
[18] S. Galli and T. Banwell, "A novel approach to the modeling of the indoor power line channel-Part II: transfer function and its properties," *IEEE Trans. on Power Delivery*, vol. 20, no.3, pp. 1869-1878, July 2005.
[19] T. Zhong, "A new power line modem and its performance in power line channels," M. S. thesis, Dept. Elect. Eng., British Columbia Univ., Vancouver, Canada, 1996.
[20] L. B. Wang, S. Lam, S. K. Yak, O. Manish, and P. T. Seng, "Investigation of radiated emissions in power line communications networks," *Int. Journal of Emerging Electric Power Systems*, vol. 9, no. 3, Article 4, 2008.
[21] Agilent EEsof EDA, Agilent Design System (ADS) version 2008, Agilent Technologies Inc, California, USA.
[22] MATLAB version R2009a, Mathworks Inc, Massachusetts, USA.
[23] CST Microwave Studio version 2011, Computer Simulation Technology, Darmstadt, Germany.

Azlan Hakimi Yahaya Rashid was born in Kuala Lumpur, Malaysia in 1984. He received the Bachelor Degree in Electrical Engineering from University Teknologi Mara, Shah Alam, Malaysia, in November 2008 and is currently working toward the M.Sc. at Universiti Teknologi Petronas, Tronoh, Perak, Malaysia.

Grant Andrew Ellis received the PhD degree in Electrical Engineering from the University of Washington, Seattle, in 1995. He has more than 25 years of professional experience in the areas of RF and Microwave design and antenna analysis and design. Dr Ellis has written over 30 papers and publications and holds 5 US patents. Dr. Ellis is the founding chairman of the IEEE MTT/ED/AP Penang Chapter. He is a registered professional engineer in the State of California and is a Senior Member of the IEEE.